

This discussion paper is/has been under review for the journal Atmospheric Chemistry and Physics (ACP). Please refer to the corresponding final paper in ACP if available.

# Automated ground-based remote sensing measurements of greenhouse gases at the Białystok site in comparison with collocated in-situ measurements and model data

J. Messerschmidt<sup>1,\*</sup>, H. Chen<sup>2,\*\*</sup>, N. M. Deutscher<sup>1</sup>, C. Gerbig<sup>2</sup>, P. Grupe<sup>1</sup>,  
K. Katrynski<sup>4</sup>, F.-T. Koch<sup>2</sup>, J. V. Lavrič<sup>2</sup>, J. Notholt<sup>1</sup>, C. Rödenbeck<sup>2</sup>, W. Ruhe<sup>3</sup>,  
T. Warneke<sup>1</sup>, and C. Weinzierl<sup>1</sup>

<sup>1</sup>Institute of Environmental Physics, University of Bremen, Bremen, Germany

<sup>2</sup>Max Planck Institute for Biogeochemistry, Jena, Germany

<sup>3</sup>impres GmbH, Bremen, Germany

<sup>4</sup>AeroMeteoservice, Białystok, Poland

32245

\*now at: California Institute of Technology, Pasadena, CA, USA

\*\*now at: NOAA-ESRL, Boulder, CO 80305, USA

Received: 14 September 2011 – Accepted: 21 November 2011 – Published: 8 December 2011

Correspondence to: J. Messerschmidt (janina@caltech.edu)

Published by Copernicus Publications on behalf of the European Geosciences Union.

32246

## Abstract

The fully automated observatory for total greenhouse gas (GHG) column measurements introduced here complements the in-situ facilities at the Białystok site in Poland. With the automated Fourier Transform Spectrometer (FTS), solar absorption measurements have been recorded nearly continuously since March 2009. In this article the automation system, including the hardware components and the automation software will be described in its basics. Furthermore the first comparison of the FTS dataset with the collocated in-situ measurements and the first comparison of the Jena CO<sub>2</sub> inversion model are presented. This model identifies monthly variations in the total CO<sub>2</sub> column and the seasonal amplitude is in good agreement with the FTS measurements.

## 1 Introduction

Until recently remote sensing measurements of greenhouse gases have not been used in atmospheric inversions to determine CO<sub>2</sub> source/sink distributions. Atmospheric inverse transport modeling have traditionally been based on a network of in-situ boundary layer measurement stations. The surface flux distributions were derived from these atmospheric concentration measurements and therewith limited by the sparse spatial coverage of the sampling sites (Marquis and Tans, 2008). Additionally, recent studies showed the sensitivity of the CO<sub>2</sub> sink estimates to the modeled vertical transport. As a result of incorrect vertical transport, a large set of atmospheric inverse model results were inconsistent with total column measurements and vertical aircraft profiles (Baker et al., 2006; Stephens et al., 2007; Yang et al., 2007). By integrating total column measurements within the existing observations, the estimation of the spatial distribution and the temporal variation of the CO<sub>2</sub> sources and sinks is expected to be improved.

Within two EU projects, GEOmon (Global Earth Observation and Monitoring of the Atmosphere) and IMECC (Infrastructure for Measurements of the European Carbon Cycle), the FTS group at the Institute of Environmental Physics (IUP) was responsible

32247

for upgrading the GHG in-situ sites at Białystok (Poland) and Trainou (France) with two automated mobile FTS instruments. These two sites are among the most important sites for GHG in-situ measurements in Europe. Currently these are the only sites in Europe where collocated FTS solar absorption and vertical resolved in-situ measurements, including tall tower and regular aircraft profiling in the boundary layer, are performed. The Białystok site is the easternmost measurement station within Europe. Besides the on-site tall tower (300 m), low aircraft profiling up to 2.8 km is operated regularly.

To measure the background abundances of trace gases, measurement sites are remote from local sources of these gases. The local infrastructure is often rudimentary and an operator only occasionally on-site. Therefore automation of the measurement system is desirable (Washenfelder et al., 2006; Deutscher et al., 2010; Geibel et al., 2010). In order to perform autonomous measurements, maintenance has to be minimized and a maximum of remote control by different remote access possibilities needs to be guaranteed. A sophisticated logging system is aimed at ensuring the system state is recorded at all times, and a basic self-organized error handling allows a minimum of local support.

In the period from August 2007 until August 2009 the FTS automation system was designed and implemented for the two FTS instruments at the IUP in Bremen in collaboration with the company impres GmbH. Different instruments were integrated to one programmable system and the automation strategy and software were developed. The automated FTS system detects the weather conditions, performs measurements along given day specific tasks, executes self-organized error handling and is entirely remote-controlled. During the installation, side-by-side measurements were performed to ensure intercomparability between instruments (Messerschmidt et al., 2010). In February 2009 the first instrument was successfully installed in Białystok, Poland and is operated in close cooperation with AeroMeteoService (Poland). The second instrument was installed at the Trainou site ( $\approx$  20 km northeast of Orléans, France) in August 2009 and is operated in close cooperation with the RAMCES team at LSCE (Gif-sur-Yvette,

32248













biosphere net ecosystem exchange (NEE) model, (White et al., 2000; Churkina and Trusilova, 2002). To estimate the ocean CO<sub>2</sub> uptake, an inversion based on ocean carbon data (Gloor et al., 2003; Mikaloff Fletcher et al., 2007) with small scale spatial and seasonal patterns, given by Takahashi et al. (2002), is used. The basic approach is as described in Rödenbeck et al. (2003), with updates described in Rödenbeck (2005) and Rödenbeck et al. (2006). The atmospheric fields and further information are available at: <http://www.bgc-jena.mpg.de/~christian.roedenbeck/download-CO2-3D/>.

In this work, the special run ana96\_v3.3, designed to provide 3-D atmospheric tracer fields, is used. Bialystok data were not used in the flux inversion, which was the basis for the analyzed fields.

## 5.1 Data analysis

Rodgers and Connor (2003) introduced a method to compare two instruments, of which one has a much higher vertical resolution than the other. This approach is used in the modification described by Wunch et al. (2010b). Only model data for which contemporary FTS measurements exist were considered. FTS measurements can only be taken during sunny weather conditions, therefore the comparison is restricted to these conditions. For each FTS measurement, the nearest model result within one hour was smoothed with the averaging kernel of the FTS measurement. The averaging kernels used for the comparison are shown in Fig. 7, color coded by solar zenith angle. The averaging kernel matrix represents the change in the retrieved X<sub>CO<sub>2</sub></sub> profile at one level  $i$  due to a perturbation to the true X<sub>CO<sub>2</sub></sub> profile at another level  $j$ . Since GFIT performs a profile scaling retrieval (PSR), the averaging kernel matrix reduces to a vector representing the sensitivity of the retrieved total column to perturbations of the partial columns at the various atmospheric levels.

The model profile data have to be integrated to column-averaged CO<sub>2</sub> dry-air mole fractions to be comparable to the FTS measurements. As the JC model does not provide a H<sub>2</sub>O profile output, the GFIT a priori H<sub>2</sub>O profile, which is based on NCEP data, is used for the integration.

32261

In Fig. 8 the integrated model data are shown compared to the FTS X<sub>CO<sub>2</sub></sub> time series. In the bottom panel, the FTS daily averages are shown in a black dotted line. The FTS time series exhibits several gaps due to bad weather conditions and instrumental problems, e.g. solar tracker failures, or internal laser breakdown. The associated daily averages of the integrated model data are indicated with a gray dotted line. In the upper panel the difference (FTS minus model data) of the daily averages is shown. The mean of the differences of  $-1.2$  ppm is given as a thin black line. Additionally, the results for the integrated low aircraft measurements, described in Sect. 5.2, are given color coded for each overpass day.

The differences between the FTS data and the model simulation are rather small, but vary periodically with time (Upper panel, Fig. 8). This indicates that to first order, the JC model captures the seasonal amplitude and phase of the column measurements well. This is challenging because it is difficult to model the biospheric uptake in Europe due to the heterogeneously distributed large variety of ecosystems in a rather small land area. The differences are, however, time-dependent and will be further investigated in a multiple year comparison. In a first investigation, the influence of local variations on the integrated model results is analyzed with on-site in-situ data.

## 5.2 The Jena CO<sub>2</sub> inversion model in comparison with the tall tower measurements

The model outputs at the five level heights of the collocated tall tower are compared with the in-situ data taken at these heights (not all shown). The CO<sub>2</sub> time series for the lowest and the highest level (5 m, 300 m) are pictured in comparison with the model results in Fig. 9. All data are given as weekly averages of daytime measurements between 12:00 p.m. and 03:00 p.m.. The Jena CO<sub>2</sub> inversion captures the seasonal cycle at both levels to the first order, whereas the higher level is better captured, especially in the winter.

The nocturnal time series for both levels are shown in Fig. 10. All data are given as weekly averages of nighttime measurements between 00:00 a.m. and 05:00 a.m.. The

32262

nocturnal seasonal cycle at 300 m is captured, whereas the model fails to modulate the nocturnal CO<sub>2</sub> accumulation at the lowest level (Fig. 10). This could be due to imperfect vertical mixing, e.g. the stable boundary layer during the night is not well represented (Fig. 6), or imperfect fluxes (false partitioning of respiration and gross primary production (GPP) but more or less reasonable net ecosystem exchange (NEE) as constrained by the inversion). If the vertical mixing is wrong, but the fluxes are correct, the 300 m model data would be increased, because the nocturnal accumulated CO<sub>2</sub> would have been transported to higher layers. The good representation of the nocturnal seasonal cycle at 300 m suggests a false partitioning of the NEE.

### 5.3 The Jena CO<sub>2</sub> inversion model in comparison with low aircraft measurements

The model simulation in the upper PBL and lower free troposphere is investigated with low aircraft profiles taken on a regular base near the Białystok site. The quality of the aircraft data is ensured by comparison to independent CO<sub>2</sub> mixing ratio measurements from an in-situ analyzer, and analyzes of flask samples collected during the flights (Chen et al., 2011). A total of 12 low aircraft profiles were available for the analyzed time period and are listed in Table 1. The measurements were taken in spirals at an average distance of 9 km (between 2 km and 13 km) to the Białystok site.

In order to compare the low aircraft profile measurements, the aircraft profiles and the model profiles are interpolated on the common pressure-grid used for the integration in Sect. 5.1. The low aircraft profiles are compared at pressure levels corresponding to the surface and altitudes of 1, 2, and 3 km to the most contemporary model profile. The time differences between the model profiles and the low aircraft profiles are listed in Table 1. In Fig. 11, the differences between the model and the aircraft profiles are shown color-coded for each of the 12 low aircraft profiles. A CO<sub>2</sub> overestimation by the original model output leads to a positive difference, and vice versa. The thick black line indicates the mean difference for all profiles. The model captures on average the CO<sub>2</sub> at the surface, but the differences have the greatest variability. In altitudes of 1 and

32263

2 km the model overestimates the CO<sub>2</sub>, whereas at 3 km the CO<sub>2</sub> is captured again on average.

To compare the total column averages, the aircraft profiles were extended above the aircraft ceiling with the most contemporary model profile. Afterwards, the extended profiles were integrated as described in Sect. 5.1. The differences between the integrated extended low aircraft profiles and the integrated most contemporary model profiles are listed in Table 1. In Fig. 8 the CO<sub>2</sub> total column averages calculated with the extended aircraft profiles are shown color coded for each overpass in comparison to the results calculated with the model profiles. Using the low aircraft measurements leads on average to a downscaling of the associated original model result. Calculated only for the overpass days, it reduces the difference of 0.81 ppm ± 0.49 ppm between the JC model and the FTS data to 0.48 ppm ± 0.79 ppm.

## 6 Conclusions

The fully automated FTS systems in Białystok was introduced. The underlying automation concept, the hardware and the software were described in their main functions. The minimization of maintenance, the safeness and robustness of the system were key factors in the automation. The automation system offers multiple remote access, as well as the possibility of filing different trace gas measurement tasks for arbitrary time periods. The safeness of the data record is guaranteed by redundant data storage. The ability of the automated system to continuously measure trace gas total columns in the near infrared is demonstrated with the FTS X<sub>CO<sub>2</sub></sub> dataset presented here.

The first comparison of the Białystok FTS dataset to collocated in-situ boundary layer CO<sub>2</sub> measurements and the Jena CO<sub>2</sub> inversion model was performed. The FTS total CO<sub>2</sub> column measurements show the expected muted seasonal cycle compared to the collocated tall tower CO<sub>2</sub> measurements due to the reduced sensitivity to the local planetary boundary layer. In comparison with the Jena CO<sub>2</sub> inversion model, it is

32264

shown that the model is able to predict monthly variations and the amplitude and the phase of the CO<sub>2</sub> seasonal cycle, despite small time dependent differences. The influence of local variations on the integrated model output was analyzed by using tall tower measurements and low aircraft profiles. The tall tower data indicate a false nocturnal respiration assumed in the JC model and the comparison to the low aircraft profiles points to an overestimation in the upper PBL, which is in agreement with the overestimation seen in the total column measurements. The use of the multiple datasets available at the Białystok site gives additional information about the performance of model simulations and thereby implicates improvements of CO<sub>2</sub> sink estimations.

*Acknowledgements.* The Białystok FTS instrument was automated with funding from the Senate of Bremen and the EU projects IMECC (Infrastructure for Measurement of the European Carbon Cycle) and GEOmon (Global Earth Observation and Monitoring). The maintenance and logistical work is kindly provided by AeroMeteo Service (Białystok) and RAMCES team at LSCE (Gif-sur-Yvette, France). We acknowledge financial support by NASA's Program, grant number NNX11AG016, Constraining fluxes of carbon with total column measurements of CO<sub>2</sub> and CH<sub>4</sub>.

## References

- Andrews, A. E., Boering, K. A., Daube, B. C., Wofsy, S. C., Loewenstein, M., Jost, H., Podolske, J. R., Webster, C. R., Herman, R. L., Scott, D. C., Flesch, G. J., Moyer, E. J., Elkins, J. W., Dutton, G. S., Hurst, D. F., Moore, F. L., Ray, E. A., Romashkin, P. A., and Strahan, S. E.: Mean ages of stratospheric air derived from in situ observations of CO<sub>2</sub>, CH<sub>4</sub>, and N<sub>2</sub>O, *J. Geophys. Res.*, 106, 32295–32314, 2001. 32257
- Baker, D. F., Law, R. M., Gurney, K. R., Rayner, P., Peylin, P., Denning, A. S., Bousquet, P., Bruhwiler, L., Chen, Y.-H., Ciais, P., Fung, I. Y., Heimann, M., John, J., Maki, T., Maksyutov, S., Masarie, K., Prather, M., Pak, B., Taguchi, S., and Zhu, Z.: TransCom 3 inversion inter-comparison: Impact of transport model errors on the interannual variability of regional CO<sub>2</sub> fluxes, 1988-2003, *Global Biogeochem. Cycles*, 20, GB1002, doi:10.1029/2004GB002439, 2006. 32247
- 32265
- Bird, R. E. and Hulstrom, R. L.: Simplified Clear Sky Model for Direct and Diffuse Insolation on Horizontal Surfaces, Technical Report SERI/TR-642-761, Solar Energy Research Institute, 1981. 32256
- Chen, H., Winderlich, J., Gerbig, C., Katrynski, K., Jordan, A., and Heimann, M.: Validation of routine continuous airborne CO<sub>2</sub> observations near the Białystok Tall Tower, *Atmos. Chem. Phys.*, accepted, 2011. 32263
- Churkina, G. and Trusilova, K.: A global version of the biome-bgc terrestrial ecosystem model, Tech. rep., Max Planck Institute for Biogeochemistry, Jena, 2002. 32261
- Deutscher, N. M., Griffith, D. W. T., Bryant, G. W., Wennberg, P. O., Toon, G. C., Washenfelder, R. A., Keppel-Aleks, G., Wunch, D., Yavin, Y., Allen, N. T., Blavier, J.-F., Jiménez, R., Daube, B. C., Bright, A. V., Matross, D. M., Wofsy, S. C., and Park, S.: Total column CO<sub>2</sub> measurements at Darwin, Australia - Ú site description and calibration against in situ aircraft profiles, *Atmos. Meas. Tech.*, 3, 947–958, doi:10.5194/amt-3-947-2010, 2010. 32248, 32258
- Geibel, M. C., Gerbig, C., and Feist, D. G.: A new fully automated FTIR system for total column measurements of greenhouse gases, *Atmos. Meas. Tech.*, 3, 1363–1375, doi:10.5194/amt-3-1363-2010, 2010. 32248
- GLOBALVIEW-CO2: Cooperative Atmospheric Data Integration Project – Carbon Dioxide, NOAA-ESRL, Boulder, Colorado, cD-ROM, 2010. 32257
- Gloor, M., Gruber, N., Sarmiento, J., Sabine, C. L., Feely, R. A., and Rödenbeck, C.: A first estimate of present and preindustrial air-sea CO<sub>2</sub> flux patterns based on ocean interior carbon measurements and models, *Geophys. Res. Lett.*, 30, 10-1–10-4, 2003. 32261
- Hase, F., Blumenstock, T., and Paton-Walsh, C.: Analysis of the Instrumental Line Shape of High-Resolution Fourier Transform IR Spectrometers with Gas Cell Measurements and New Retrieval Software, *Appl. Optics*, 38, 3417–3422, 1999. 32252
- Heimann, M. and Koerner, S.: The global atmospheric tracer model TM3, Technical Report 5, Max-Planck-Institut für Biogeochemie, 2003. 32260
- Keppel-Aleks, G., Toon, G. C., Wennberg, P. O., and Deutscher, N. M.: Reducing the impact of source brightness fluctuations on spectra obtained by Fourier-transform spectrometry, *Appl. Optics*, 46, 4774–4779, 2007. 32256
- Marquis, M. and Tans, P.: Carbon Crucible, *Science*, 320, 460–461, 2008. 32247
- Messerschmidt, J., Macatangay, R., Notholt, J., Petri, C., Warneke, T., and Weinzierl, C.: Side by side measurements of CO<sub>2</sub> by ground-based Fourier transform spectrometry (FTS), *Tellus B*, 62, 749–758, doi:10.1111/j.1600-0889.2010.00491.x, 2010. 32248, 32258

- Messerschmidt, J., Geibel, M. C., Blumenstock, T., Chen, H., Deutscher, N. M., Engel, A., Feist, D. G., Gerbig, C., Gisi, M., Hase, F., Katrynski, K., Kolle, O., Lavric, J. V., Notholt, J., Palm, M., Ramonet, M., Rettinger, M., Schmidt, M., Sussmann, R., Toon, G. C., Truong, F., Warneke, T., Wennberg, P. O., Wunch, D., and Xueref-Remy, I.: Calibration of TCCON column-averaged CO<sub>2</sub>: the first aircraft campaign over European TCCON sites, *Atmos. Chem. Phys.*, 11, 10765–10777, doi:10.5194/acp-11-10765-2011, 2011. 32258
- Mikaloff Fletcher, S. E., Gruber, N., Jacobson, A. R., Gloor, M., Doney, S. C., Dutkiewicz, S., Gerber, M., Follows, M., Joos, F., Lindsay, K., Menemenlis, D., Mouchet, A., Müller, S. A., and Sarmiento, J. L.: Inverse estimates of the oceanic sources and sinks of natural CO<sub>2</sub> and the implied oceanic carbon transport, *Global Biogeochem. Cycles*, 21, GB1010, doi:10.1029/2006GB002751, <http://dx.doi.org/10.1029/2006GB002751>, 2007. 32261
- Olivier, J. G. J. and Berdowski, J. J. M.: The Climate System, chap. Global emissions sources and sinks, pp. 33–78, Publishers/Swets & Zeitlinger Publishers, Lisse, The Netherlands, ISBN: 90-5809-255-0, 2001. 32260
- Popa, M. E., Gloor, M., Manning, A. C., Jordan, A., Schultz, U., Haensel, F., Seifert, T., and Heimann, M.: Measurements of greenhouse gases and related tracers at Bialystok tall tower station in Poland, *Atmospheric Measurement Techniques*, 3, 407–427, doi:10.5194/amt-3-407-2010, 2010. 32259
- Rödenbeck, C.: Estimating CO<sub>2</sub> sources and sinks from atmospheric mixing ratio measurements using a global inversion of atmospheric transport, Technical report 6, Max Planck Institute for Biogeochemistry, Jena, 2005. 32260, 32261
- Rödenbeck, C., Houweling, S., Gloor, M., and Heimann, M.: CO<sub>2</sub> flux history 1982–2001 inferred from atmospheric data using a global inversion of atmospheric transport, *Atmos. Chem. Phys.*, 3, 1919–1964, doi:10.5194/acp-3-1919-2003, 2003. 32261
- Rödenbeck, C., Conway, T. J., and Langenfelds, R.: The effect of systematic measurement errors on atmospheric CO<sub>2</sub> inversions: a quantitative assessment, *Atmos. Chem. Phys. Discuss.*, 5, 8979–9001, doi:10.5194/acpd-5-8979-2005, 2005. 32261
- Rodgers, C. D. and Connor, B. J.: Intercomparison of remote sounding instruments, *J. Geophys. Res.*, 108, 13-1–13-14, 2003. 32261
- Rothman, L., Gordon, I., Barbe, A., Benner, D., Bernath, P., Birk, M., Boudon, V., Brown, L., Campargue, A., Champion, J.-P., Chance, K., Coudert, L., Dana, V., Devi, V., Fally, S., Flaud, J.-M., Gamache, R., Goldman, A., Jacquemart, D., Kleiner, I., Lacombe, N., Lafferty, W., Mandin, J.-Y., Massie, S., Mikhailenko, S., Miller, C., Moazzen-Ahmadi, N., Naumenko, O.,

32267

- Nikitin, A., Orphal, J., Perevalov, V., Perrin, A., Predoi-Cross, A., Rinsland, C., Rotger, M., Simecková, M., Smith, M., Sung, K., Tashkun, S., Tennyson, J., Toth, R., Vandaele, A., and Auwera, J. V.: The HITRAN 2008 molecular spectroscopic database, *J. Quant. Spectrosc. Ra.*, 110, 533–572, doi:10.1016/j.jqsrt.2009.02.013, *HiTRAN*, 2009. 32257, 32275
- Stephens, B. B., Gurney, K. R., Tans, P. P., Sweeney, C., Peters, W., Bruhwiler, L., Ciais, Philippe AN DRamonet, M., Bousquet, P., Nakazawa, T., Aoki, S., Machida, T., Inoue, G., Vinnichenko, N., Lloyd, J., Jordan, A., Heimann, M., Shibistova, O., Langenfelds, Ray L., Steele, L. P., Francey, R. J., and Denning, A. S.: Weak Northern and Strong Tropical Land Carbon Uptake from Vertical Profiles of Atmospheric CO<sub>2</sub>, *Science*, 316, 1732–1735, doi:10.1126/science.1137004, 2007. 32247
- Takahashi, T., Sutherland, S., Sweeney, C., Poisson, A., Metzl, N., Tilbrook, B., Bates, N., Wanninkhof, R., Feely, R., Sabine, C., and Olafsson, J., and Nojiri, Y.: Global sea-air CO<sub>2</sub> flux based on climatological surface ocean pCO<sub>2</sub>, and seasonal biological and temperature effects Global sea-air CO<sub>2</sub> flux based on climatological surface ocean pCO<sub>2</sub>, and seasonal biological and temperature effects, *Deep-Sea Res. Pt. II*, 49, 1601–1622, 2002. 32261
- Washenfelder, R., Toon, G., Blavier, J.-F., Yang, Z., Allen, N., Wennberg, P., Vay, S., Matross, D., and Daube, B.: Carbon dioxide column abundances at the Wisconsin Tall Tower site, *J. Geophys. Res.*, 111, 1–11, doi:10.1029/2006JD007154, 2006. 32248, 32258
- White, M. A., Thornton, P. E., Running, S. W., and Nemani, R. R.: Parameterization and Sensitivity Analysis of the BIOME-BGC Terrestrial Ecosystem Model: Net Primary Production Controls, *Earth Interact.*, 4, 1–85, 2000. 32261
- Wunch, D., Toon, G. C., Blavier, J.-F. L., Washenfelder, R., Notholt, J., Connor, B. J., Griffith, D. W. T., Sherlock, V., and Wennberg, P. O.: The Total Carbon Column Observing Network Debra Wunch, Geoffrey C. Toon, Jean-François L. Blavier, Rebecca A. Washenfelder, Justus Notholt, Brian J. Connor, David W. T. Griffith, Vanessa Sherlock and Paul O. Wennberg, *Phil. Trans. R. Soc. A* 2011 369, 2087–2112, doi:10.1098/rsta.2010.0240, 2010a. 32257, 32258
- Wunch, D., Toon, G. C., Wennberg, P. O., Wofsy, S. C., Stephens, B. B., Fischer, M. L., Uchino, O., Abshire, J. B., Bernath, P., Biraud, S. C., Blavier, J.-F. L., Boone, C., Bowman, K. P., Browell, E. V., Campos, T., Connor, B. J., Daube, B. C., Deutscher, N. M., Diao, M., Elkins, J. W., Gerbig, C., Gottlieb, E., Griffith, D. W. T., Hurst, D. F., Jiménez, R., Keppel-Aleks, G., Kort, E. A., Macatangay, R., Machida, T., Matsueda, H., Moore, F., Morino, I., Park, S., Robinson, J., Roehl, C. M., Sawa, Y., Sherlock, V., Sweeney, C., Tanaka, T., and Zondlo, M. A.: Calibration of the Total Carbon Column Observing Network using aircraft profile data,

32268

- Atmos. Meas. Tech., 3, 1351–1362, doi:10.5194/amt-3-1351-2010, 2010b. 32258, 32261
- Wunch, D., Toon, G. C., Blavier, J.-F. L., Washenfelder, R. A., Notholt, J., Connor, B. J., Griffith, D. W. T., Sherlock, V., and Wennberg, P. O.: The Total Carbon Column Observing Network, Philos. T. R. Soc. A, 369, 2087–2112, doi:10.1098/rsta.2010.0240, <http://rsta.royalsocietypublishing.org/content/369/1943/2087.abstract>, 2011. 32252
- 5 Yang, Z., Washenfelder, R., Keppel-Aleks, G., Krakauer, N., Randerson, J., Tans, P., Sweeney, C., and Wennberg, P.: New constraints on Northern Hemisphere growing season net flux, Geophys. Res. Lett., 34, L12807, doi:10.1029/2007GL029742, 2007. 32247

32269

**Table A1.** Low aircraft overpasses available for the analyzed time period at the Bialystok site. The date, the time difference to nearest available model output, the distance and altitude range are listed. The last column shows the difference between the integrated extended low aircraft profiles and the integrated most contemporary model result.

date [dd-mmm HH:MM-HH:MM]	$\Delta t$ (JC-in-situ) [HH:MM]	dist. range [km]	alt. range [km]	$\Delta$ (JC- assembled JC) [ppm]
31 Mar, 14:09–15:21	02:09	2.44–13.32	0.09–2.47	0.00
8 Apr, 08:48–10:06	02:48	1.74–12.28	0.09–2.52	–0.44
27 Apr, 15:35–16:53	03:35	2.58–13.49	0.09–2.53	0.25
15 May, 14:45–15:51	08:45	1.24–13.07	0.08–2.47	0.41
29 May, 10:29–11:30	–00:30	1.21–52.50	0.12–2.54	0.13
15 Jun, 11:44–12:56	00:00	0.92–14.04	0.09–2.62	0.68
29 Jun, 11:08–12:09	00:00	2.24–13.08	0.11–2.67	0.43
7 Jul, 10:29–11:42	–00:15	2.54–13.15	0.07–2.63	–0.05
18 Jul, 08:51–10:04	01:56	2.55–13.38	0.11–2.65	2.21
10 Aug, 13:10–14:18	–16:49	2.15–17.59	0.11–2.79	1.09
25 Aug, 11:30–11:38	–00:22	3.04–13.83	0.10–0.34	–0.42
27 Nov, 11:13–11:49	–00:11	2.64–13.00	0.10–1.47	–0.36

32270



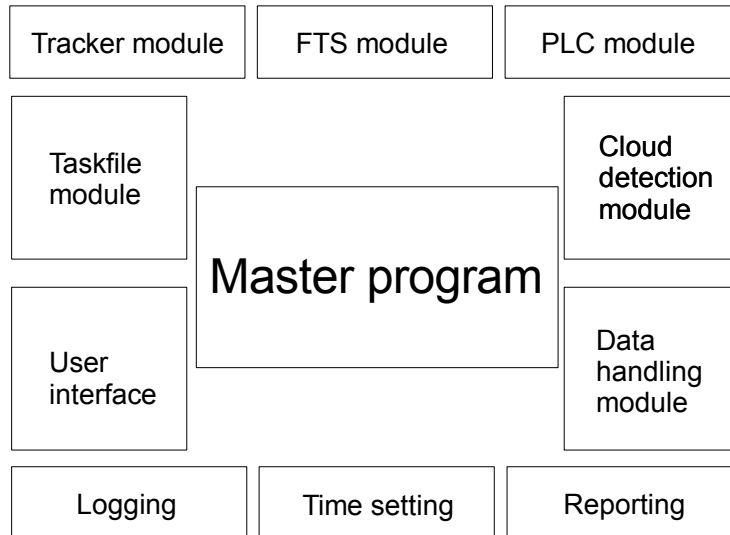


**Fig. 2.** Schematic of the interacting modules within the automation software. The fact that the Master Program is central to the function of the software is evident. At the top the major modules for the measurement process are shown. On the right, supplemental modules for the measurement process are grouped. On the left, the provided modules for the local and remote access are indicated. At the bottom, logging tools and the time setting are summarized.

32273

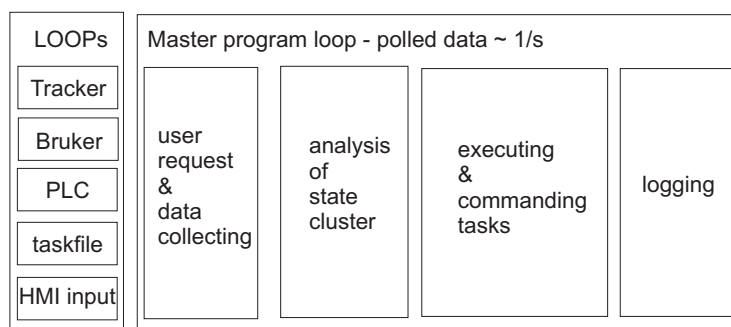


**Fig. 3.** The basic dynamical structure of the automation program. All submodules provide the update of their parameters in a loop process. The Master program itself is set up in a loop process. It checks for local or remote user requests, collects the provided information of the submodules and analyzes these information. By commanding tasks to the subsystems, it executes subsequent actions. At the end of one loop, it logs all information as the state of the automation system.

32274

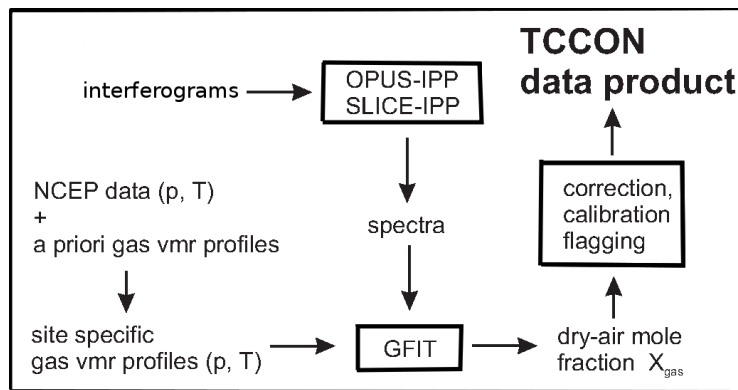


**Fig. 4.** The software used for the retrieval of atmospheric column-averaged dry-air mole fractions. The main processes are outlined: The measured interferograms are transformed into spectra with the OPUS-IPP or SLICE-IPP software. The a priori profile is approximated with NCEP/NCAR analysis data for the measurement site and day. In GFIT the initial vertical gas mole fraction profile, the a priori profile, is scaled to fit best spectra e.g. of the HITRAN database (Rothman et al., 2009). After correction, calibration and data flagging, the TCCON product are column-averaged dry-air mole fractions  $X_{\text{gas}}$ .

32275

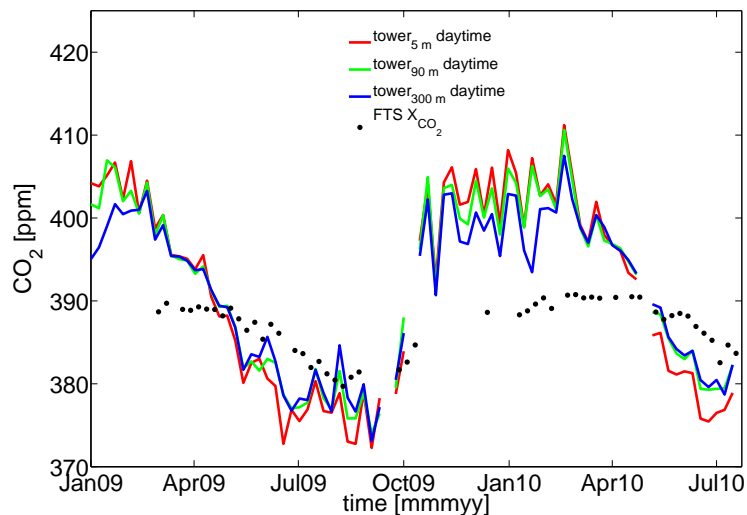


**Fig. 5.** The daytime  $\text{CO}_2$  time series for three tall tower levels (5 m, 90 m, 300 m) highlighting the seasonal cycle in comparison with the FTS measurements. All measurements are shown as weekly averages of daytime measurements between 12:00 p.m. and 03:00 p.m. local time. Gaps in the in-situ data record are due to instrumental problems.

32276

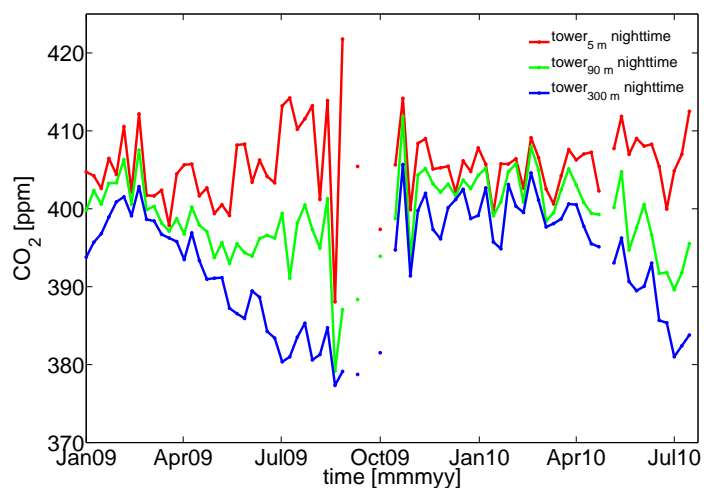


**Fig. 6.** The nocturnal CO<sub>2</sub> time series for three tall tower levels (5 m, 90 m, 300 m) highlighting the seasonal cycle. The measurements are shown as weekly averages of nighttime measurements between 00:00 am and 05:00 am local time. Gaps in the in-situ data record are due to instrumental problems.

32277

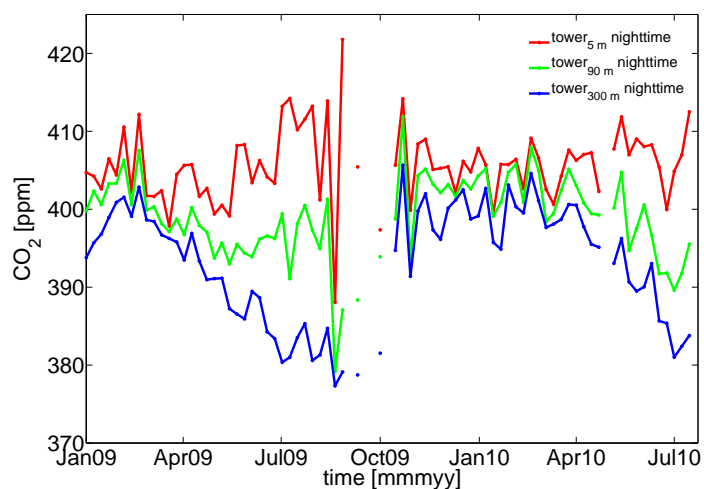


**Fig. 7.** CO<sub>2</sub> averaging kernels for the presented Białystok FTS measurements color coded for different solar zenith angles. The averaging kernels have no distinct maximum and are constant to first approximation within the troposphere and vary primarily due to different solar zenith angles.

32278

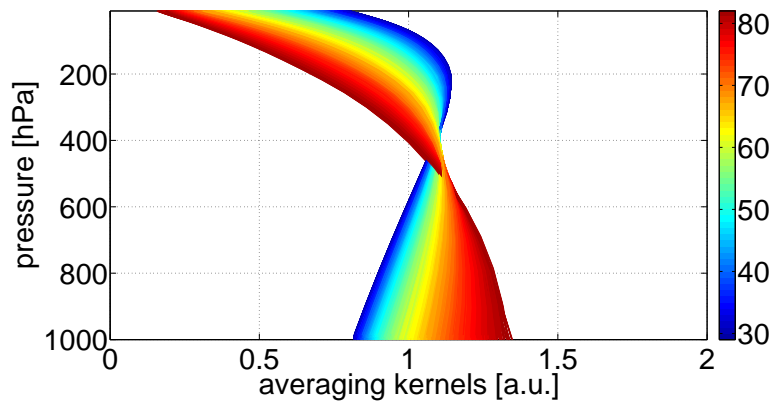


**Fig. 8.** Upper panel: The difference between the Bialystok FTS daily averages and the corresponding integrated model data. The black line indicates the mean difference. The integrated low aircraft measurements, extended above the aircraft ceiling by the model are given color coded for the different overpasses (Sect. 5.2). Bottom panel: the integrated model data of the Jena CO<sub>2</sub> inversion (JC) in comparison with the FTS time series.

32279

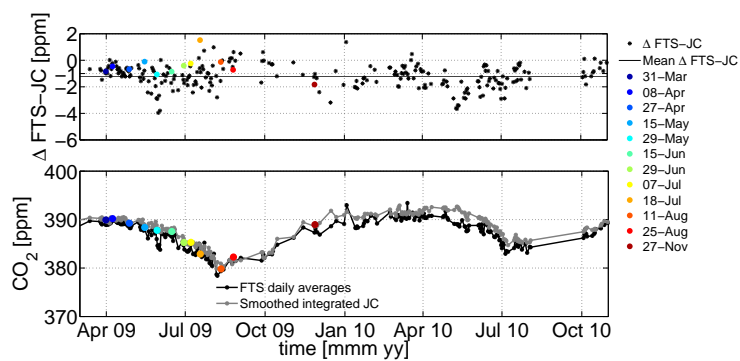


**Fig. 9.** The JC model output at the lowest and highest level of the tall tower (5 m, 300 m). Weekly averages of daytime measurements between 12:00 p.m. and 03:00 p.m. are compared. The Jena CO<sub>2</sub> inversion captures the seasonal cycle at both levels to the first order, whereas especially in the winter the higher level is better captured.

32280

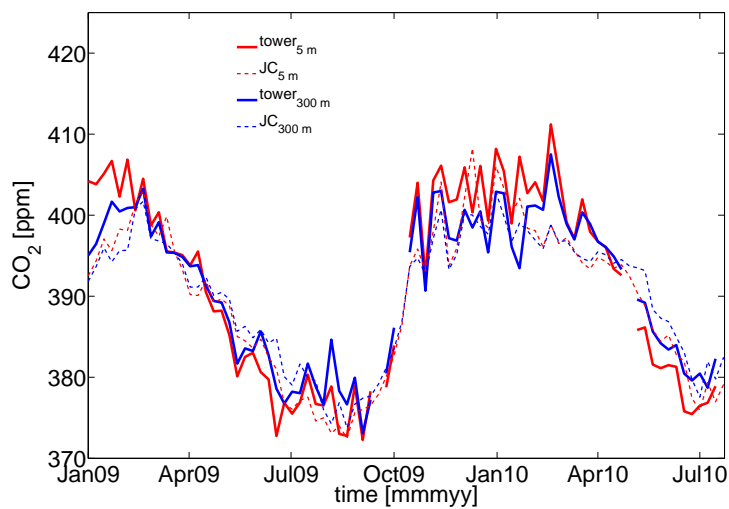


**Fig. 10.** The JC model output at the lowest and highest level of the tall tower (5 m, 300 m). Weekly averages of nighttime measurements between 00:00 a.m. and 05:00 a.m. are compared. The model captures the seasonal cycle at the upper level, but fails to simulate the nighttime CO<sub>2</sub> accumulation at the ground.

32281

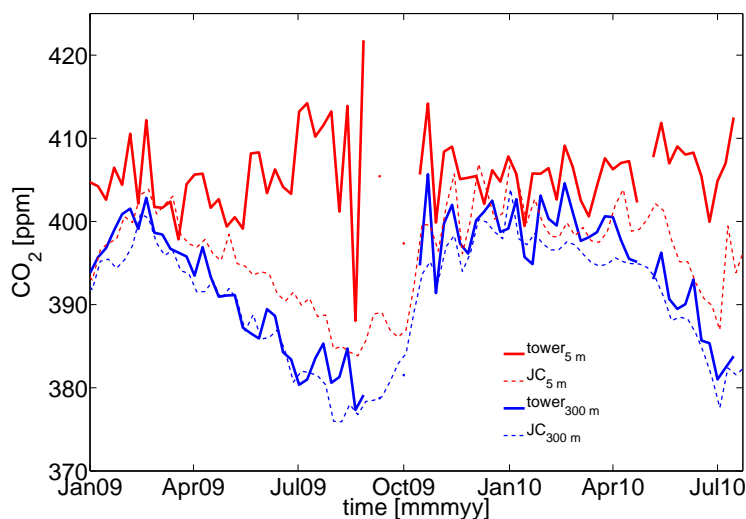


**Fig. 11.** Difference between the model profiles and contemporary low aircraft profiles on the common pressure-grid used for the integration in Sect. 5.1. For the analyzed time period overall 12 low aircraft profiles up to 2.8 km were conducted, shown color-coded for each overpass. The mean of the differences is given with a black line. At the ground and in 3 km, the JC model captures the CO<sub>2</sub> on average and significantly overestimates it in 1 and 2 km.

32282